ACADEMIC
PRESS

Identifying regional activity associated with temporally separated components of working memory using event-related functional MRI

Dara S. Manoach,[a,c,d,]* Douglas N. Greve,[b,c,d] Kristen A. Lindgren,[a,d] and Anders M. Dale[b,c,d]

[a] *Department of Psychiatry, Massachusetts General Hospital, Charlestown, MA 02129, USA*
[b] *Department of Radiology, Massachusetts General Hospital, Charlestown, MA 02129, USA*
[c] *Athinoula A. Martinos Center, Charlestown, MA 02129, USA*
[d] *Harvard Medical School, Boston, MA 02215, USA*

Abstract

This study describes the neural circuitry underlying temporally separated components of working memory (WM) performance—stimulus encoding, maintenance of information during a delay, and the response to a probe. While other studies have applied event-related fMRI to separate epochs of WM tasks, this study differs in that it employs a methodology that does not make any a priori assumptions about the shape of the hemodynamic response (HDR). This is important because no one model of the HDR is valid across the range of activated brain regions and stimulus types. Systematic modeling inaccuracies may lead to the misattribution of activity to adjacent events. Twelve healthy subjects performed a numerical version of the Sternberg Item Recognition Paradigm adapted for rapid presentation event-related fMRI. This paradigm emphasized maintenance rather than manipulative WM processes and used a subcapacity WM load. WM trials with different delay lengths were compared to fixation. The HDR of the entire WM trial for each trial type was estimated using a finite impulse response (FIR). Regional activity associated with the Encode, Delay, and Probe epochs was identified using contrasts that were based on the FIR estimates and by examining the HDRs. Each epoch was associated with a distinct but overlapping pattern of regional activity. Activation of the dorsolateral prefrontal cortex, thalamus, and basal ganglia was exclusively associated with the probe. This suggests that frontostriatal neural circuitry participates in selecting an appropriate response based on the contents of WM.
© 2003 Elsevier Inc. All rights reserved.

Introduction

Working memory (WM) is not a unitary construct. It involves distinct processes, operates on different domains of information, and can be divided into epochs with different cognitive requirements. Neuroimaging findings support a regional specialization within the prefrontal cortex (PFC) for maintenance vs manipulation processes (D'Esposito et al., 1999; Petrides, 1995) and for the different domains of information represented in WM (e.g., spatial vs nonspatial features) (D'Esposito et al., 1998). Rather than reflecting an

absolute segregation of function, however, recent evidence suggests that this regional specialization may be more a matter of degree of participation (D'Esposito et al., 1999; Haxby et al., 2000; Nystrom et al., 2000; Postle et al., 1999). The goal of the present study was to describe the neural circuitry underlying performance during each epoch of a WM task: stimulus encoding, maintenance during a delay, and the response to a probe. While other studies have applied event-related fMRI to separate the components of working memory, the present study differs in that we estimate hemodynamic responses (HDRs) using methods that are unbiased by a priori assumptions about their shape. The rationale for this approach is described below. We chose a numerical WM task that emphasizes maintenance (Sternberg Item Recognition Paradigm, SIRP) and adapted it to a rapid presentation, event-related fMRI task design. Regions

* Corresponding author. Massachusetts General Hospital, Charlestown Navy Yard, 36 First Avenue, Room 420, Charlestown, MA 02129. Fax: +1-617-726-0504.
E-mail address: dara@nmr.mgh.harvard.edu (D.S. Manoach).

that are reliably activated by the SIRP include the dorsolateral prefrontal cortex (DLPFC), intraparietal sulcus (IPS), lateral premotor cortex, supplementary motor area (SMA), and insula (Manoach et al., 1997, 1999, 2000; Rypma et al., 1999). In this study we elucidated the temporal course of their participation.

Studying the individual components of WM performance with event-related fMRI poses several experimental design and analysis challenges. The nature of WM tasks is such that the events of interest (encode, delay, probe) must be presented in an invariant order, immediately adjacent to one another in time. Although each event is discrete, the associated blood oxygenation level dependent (BOLD) response to each event overlaps. Presenting the events in a random order results in differential overlap of the residual activation from preceding events and thereby allows the contribution of each event to the aggregate response to be accurately modeled (Burock and Dale, 2000). However, because the encode, delay, and probe epochs of WM tasks cannot be randomized, different design and analysis strategies are required.

Several strategies to isolate activation due to WM components have been employed. One involves extending the length of the delay epoch so that the residual HDR to encode decays (Chein and Fiez, 2001; Cohen et al., 1997; Jha and McCarthy, 2000; Leung et al., 2002; Rypma and D'Esposito, 1999). This strategy isolates activity specific to delay processes. However, the HDR to a particular event has been estimated to take between 10 and 14 s to return to baseline (e.g., Dale and Buckner, 1997; Savoy, 2001) and the additional time required limits the number of trials that can be presented. Fewer trials may result in reduced power to detect meaningful delay-related activity. The additional time may also lead to the use of different maintenance strategies and leave room for distraction, particularly in pathological populations that are characterized by deficits in sustained attention.

Some studies have varied the WM load in order to identify regions associated with WM maintenance during a delay period (Cohen et al., 1997; Jha and McCarthy., 2000; Rypma and D'Esposito, 1999). Although this strategy identifies regions that are responsive to load, it has several limitations. Any regions involved in maintenance that are not sensitive to load will be omitted. This strategy may also identify regions that are related to the strategic processing necessary to manage supracapacity loads rather than WM maintenance per se (D'Esposito et al., 1998). In addition, regional activity during encoding may also be sensitive to load (Rypma and D'Esposito, 1999), so a long delay period is necessary to isolate delay-related activity.

Another strategy for dealing with overlap is to assume a form to the HDR for each epoch and thereby explicitly model and remove the overlap (Jha and McCarthy, 2000; Postle et al., 2000; Rowe and Passingham, 2001; Rypma and D'Esposito, 1999). While this is a statistically powerful technique when the models are correct, imposing any as-

sumed form on the HDR produces biased estimates of the true response because a single assumed models is unlikely to be valid across the range of activated brain regions and possible stimulus types (Duann et al., 2002). Systematic model inaccuracies may lead to the misattribution of activity to adjacent events as is demonstrated in Fig. 1. In addition, information about the response to each epoch is conveyed not only by the amplitude of the HDR, but by its shape. For example, areas that maintain information over a delay should show a relatively sustained response, while those involved in responding to a probe should be more transient. Therefore it is important to estimate these responses without making prior assumptions about their shape (Ollinger et al., 2001a, 2001b).

In the present study, we employed finite impulse response (FIR) models to identify regional activation associated with each of the three epochs of the WM task. FIR models do not make any a priori assumptions about the shape of the HDR. Linear models are used to estimate the response amplitude at each time point of the HDR (see Burock and Dale, 2000 for details of this technique). The FIR model protects against false positives that can be caused by modeling error when there is fixed timing between events (Fig. 1), but are usually less statistically powerful than when a HDR is assumed. Our adaptation of the SIRP was comprised of three types of WM trials that were identical except with respect to the length of the delay epoch. The delay lengths were varied to allow a separation of regional activity associated with each epoch. They were kept relatively short (0, 2, and 4 s) to minimize the possibility of distraction and the generation of different maintenance strategies. A relatively low WM load (five digits) was chosen to minimize the necessity for strategic processing during the delay period. We analyzed the data by first estimating the response to an entire trial (consisting of Encode, Delay, and Probe epochs) as a single event using a FIR model. We estimated the parameters of each of the three WM trial types (with 0, 2, and 4 s delay lengths) vs a fixation baseline. Using the results of the FIR techniques, we employed contrasts to disambiguate the HDRs to Encode, Delay, and Probe epochs. These contrasts compared the different WM trial types and the amplitudes of the HDR at different time points following the trial onset (Fig. 2). Examination of the HDR time courses provided further validation of the findings.

Materials and methods

Subjects

Twelve healthy subjects (six male, six female; mean age = 29.7 ± 6.9), without a history of psychiatric illness were recruited from the hospital community. All subjects were screened to exclude substance abuse or dependence within the past 6 months, a history of significant head injury,
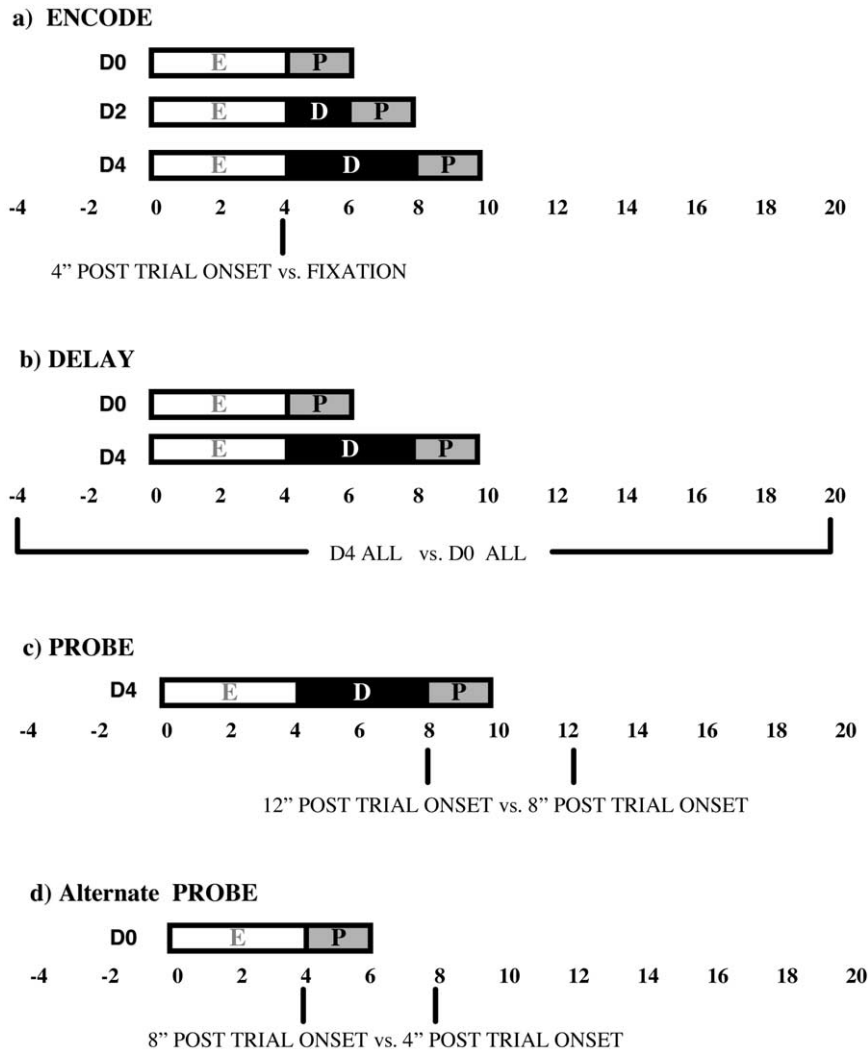
a)

b)
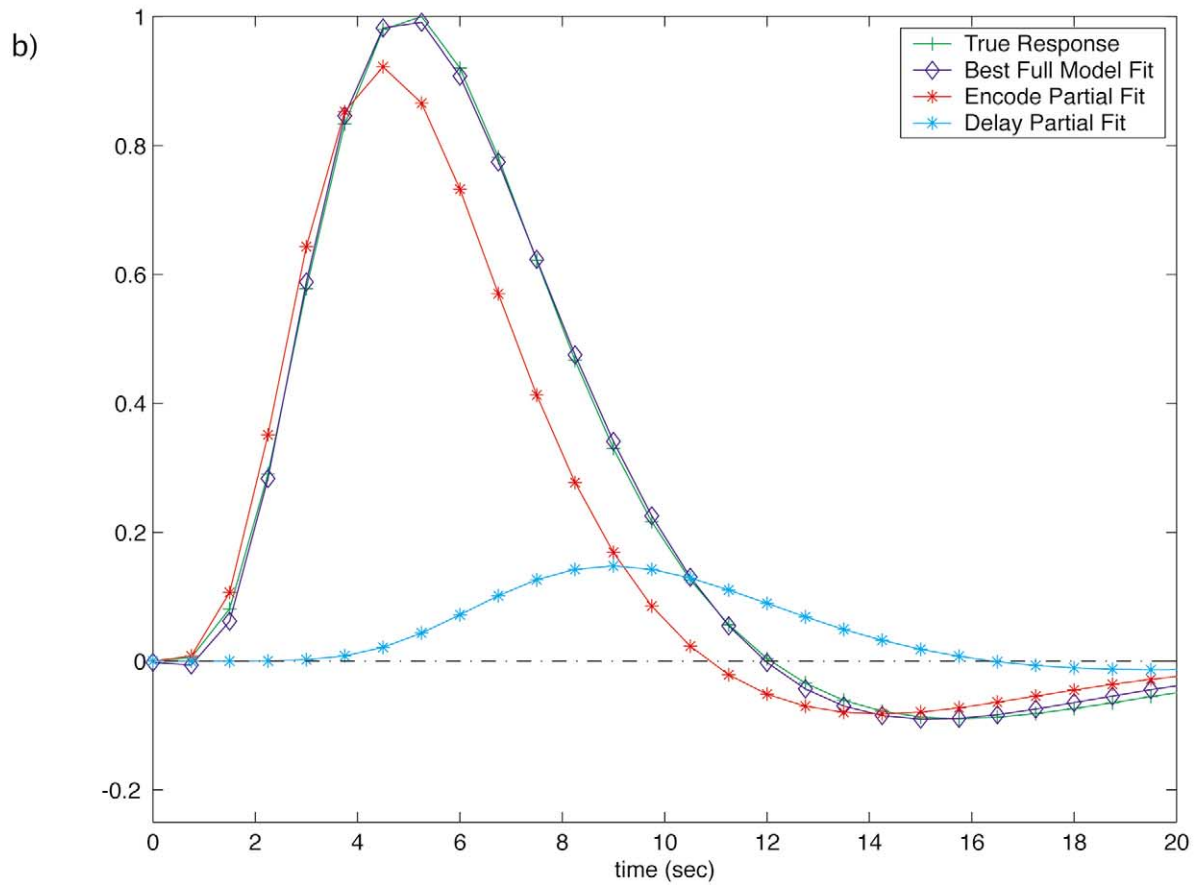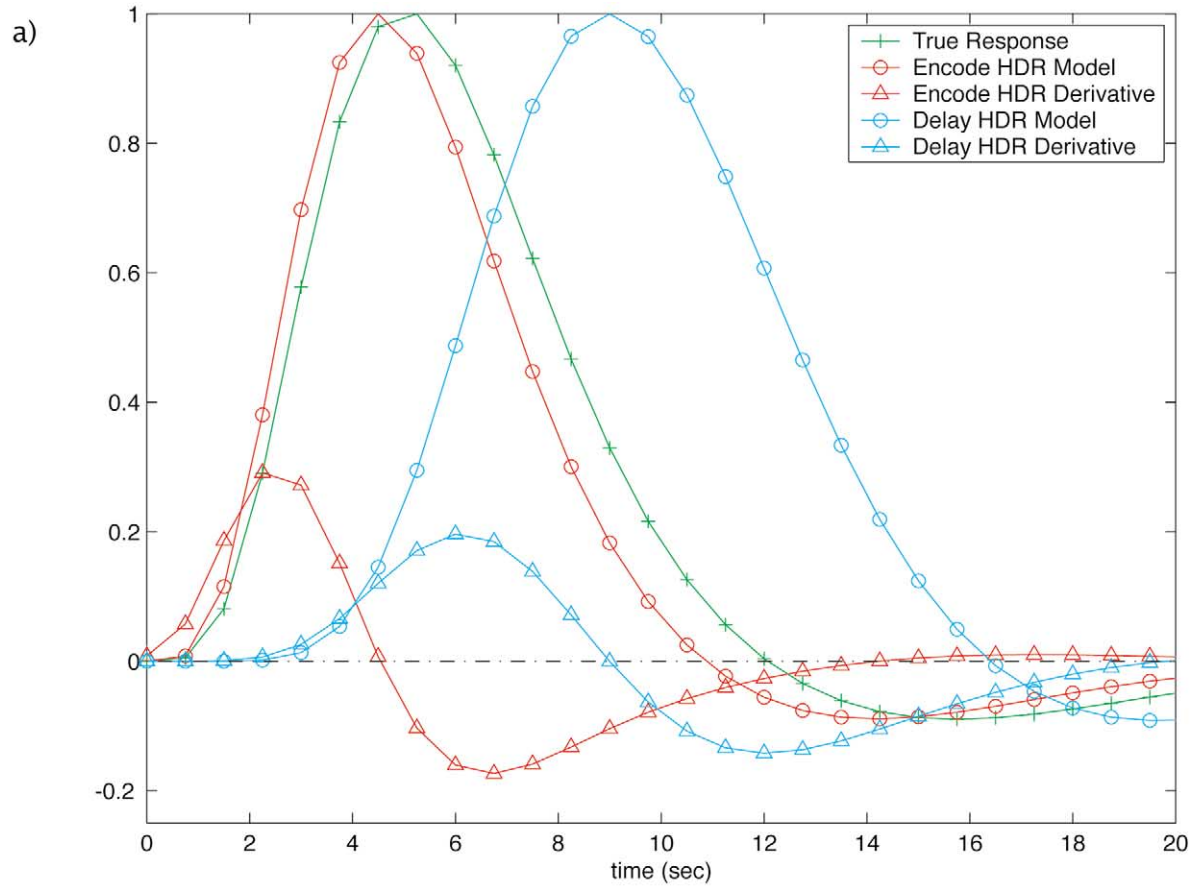
Fig. 2. The timing (in seconds) of the epochs in the three WM trial types (D0, D2, D4) and how the trials were used in contrasts designed to identify regional activation for each epoch. (a) The Encode contrast used all three trial types and compared activity at 4 s posttrial onset to the fixation baseline. (b) In the Delay contrast activity was averaged across all time points in D4 trials and was compared to the averaged activity of D0 trials. (c) The Probe contrast used only D4 trials and compared the activity at 12 s posttrial onset to activity at 8 s posttrial onset. (d) The alternate probe contrast used only D0 trials and compared the activity at 8 s posttrial onset to activity at 4 s posttrial onset.

current psychoactive medication use, and psychiatric or neurological illness. All subjects were strongly right-handed as determined by a laterality score of 70 or above on the modified Edinburgh Handedness Inventory (White and Ash-ton, 1976). Subjects had a mean of 18.6 ± 4 years of education and a mean estimated verbal IQ score of 112.5 ± 9 on the ANART (American National Adult Reading Test) (Blair and Spreen, 1989). All subjects gave written in-

Fig. 1. The misattribution of activation to an adjacent event when the form of the hemodynamic response (HDR) is assumed. In working memory paradigms both the sequence of events (Encode, Delay, Probe) and their timing is often fixed. This type of design results in a substantially increased rate of false positives (e.g., finding significant activation where there is none) if the shape of the HDR is specified. (a) For example, consider a simulation in which the true response to the Encode, Delay, and Probe sequence (lasting 4, 2, and 2 s, respectively in this example) only consists of a response to Encode (i.e., the voxel does not respond to delay or probe). However, the model of the HDR at that voxel must include components for each epoch. The HDR models for Encode and Delay and their first derivatives are shown (the Probe model is omitted for clarity of illustration). In this simulation, the shape of the assumed HDR model for Encode does not fit the true response perfectly (the dispersion of the HDR in the true response is 1.0 but is 0.9 in the model). The result of using these four regressors (HDR models and derivatives) to fit the true response is shown in b. The best full model fit to the true response is almost perfect. However, the component due to the Encode HDR model is only 92% of the true Encode response. Moreover, this analysis assigns a response to Delay even though there was no true response to delay (the amplitude of the estimated response to delay is 15% of the estimated response to Encode). This misattribution of activity during the delay results from both the difference between the true Encode response and its model, and the fixed interval between the onset of the Encode and Delay epochs. FIR estimates of the HDR protect against this misattribution of activity but may result in decreased statistical power.

Table 1
Brain regions showing significant activation in the contrasts for Encode, Delay, and Probe

Activated regions (local maxima)	BA	Encode				Delay				Probe			*P*
		x	*y*	*z*	*P*	*x*	*y*	*z*	*P*	*x*	*y*	*z*	
Encode only													
Left													
Calcarine s. (#13)	17	**−8**	**−86**	**18**	**7.1**								
Lat. occipital s.	18	−24	−86	11	6.7								
Occipiotemporal s.	19/37	−47	−67	−5	6.5								
Asc. IPS (#4)	7/40	**−34**	**−52**	**41**	**5.0**								
Right													
Fusiform g. (#16)	18	**26**	**−76**	**−4**	**6.0**								
Fusiform g.	19	35	−62	−12	5.5								
Calcarine s. (#17)	17	**14**	**−73**	**19**	**5.2**								
Asc. IPS	7/40	30	−52	40	3.8								
Encode and Delay													
Left													
Lingual g. (#14)	18	**−16**	**−68**	**−2**	**5.2**	−16	−65	−5	3.9				
Pareitooccipital s.	7/19	−24	−71	26	5.7	−17	−92	26	4.7				
Right													
Lingual g.	18	10	−65	−1	4.2	17	−67	−6	3.5				
Parietooccipital s.	7/19	28	−73	29	5.5	24	−81	28	4.2				
Med. occipital g.	19	28	−90	26	6.9	20	−89	27	4.0				
Cuneus	18	9	−91	21	5.4	15	−81	32	3.5				
Encode, delay and probe													
Left													
Sup. frontal g. (#9)	6	**−6**	**−2**	**56**	**5.9**	**−3**	**−3**	**59**	**3.8**	−6	11	53	5.0
Precentral g. (#12)	6	**−44**	**0**	**34**	**4.4**	−32	2	48	3.1	−52	5	33	5.1
Precentral g. (#2)	4	**−45**	**−11**	**49**	**6.6**	**−48**	**−11**	**44**	**4.5**	−19	−15	65	6.4
Encode and Probe													
Left													
Fusiform g. (#15)	19/18	**−36**	**−64**	**−8**	**7.8**					−29	−86	2	3.4
Right													
Sup. frontal g.	6	14	−1	58	3.9					9	−12	54	6.4
Precentral s.	6	25	−4	44	3.4					32	−2	46	4.3
Delay and Probe													
Left													
Postcentral g. (#8)	2/1					−53	−17	43	4.4	−60	−20	36	5.4
Right													
Postcentral g.	1					57	−9	39	3.4	47	24	60	6.6
Probe only													
Left													
Supramarginal g.	41									−50	−22	15	7.1
Des. IPS (#3)	2/40									**−33**	**−28**	**42**	**7.1**
Insula (#7)										**−28**	**19**	**−1**	**6.5**
Circular s. insula										−46	−5	10	6.5
Cingulate s.	6/24									−6	−5	48	6.4
Sylvian fissure	40									−46	−37	25	6.3
Thalamus (#18)										**−4**	**−23**	**5**	**5.8**
Central s.	4/3									−31	−18	50	5.7
Thalamus										−13	−9	10	5.5
Post. cingulate s.	7									−18	−39	46	4.9
Heschl's gyrus	41									−45	−21	8	4.5
Arcuate orbital s.	39									−39	−50	14	4.5
Sup. parietal lobule	5									−26	−44	56	4.2
Lenticular nucleus (#20)										**−13**	**−2**	**2**	**4.0**
Inf. frontal g.	9/44									−47	12	24	3.6
Subparietal s.	7									−6	−56	47	3.6
Inf. frontal s. (#6)	45									**−34**	**19**	**23**	**3.3**
Mid. frontal g. (#1)	9									**−34**	**22**	**32**	**3.1**

Table 1 (continued)

Activated regions (local maxima)	BA	Encode			Delay					Probe				P
		x	y	z	P	x	y	z	P	x	y	z	
Right														
Sylvian fissure	40									42	**−35**	21		6.7
Sup. frontal g.	8									12	17	45		6.3
Inf. frontal g.	44									48	9	16		6.0
Sup. parietal lobule	7									41	**−51**	59		5.9
Des. IPS	7/40									43	−34	**31**		5.8
Post. sup. temporal g.	22									65	−39	25		5.4
Cingulate s. (#11)	32/24									**12**	**2**	**39**		**5.3**
Insula										31	18	1		5.2
Circular s. insula	45/47									40	19	12		5.2
Thalamus (#19)										**9**	**−13**	**2**		**4.8**
Thalamus										7	−20	3		**4.8**
Ant. occipital s.	19/37									49	−55	8		4.7
Precentral s.	44/8									51	8	27		4.6
Fusiform g.	20									41	−20	−19		4.6
Inf. parietal lobule	40									52	−39	44		4.2
Parieto-occipital s.	31/7									18	−64	31		4.0
Mid. frontal g. (#5)	9/46									**40**	**48**	**16**		**3.7**
Sup. temporal g.	22									55	−12	**1**		3.5
Precuneus	7									14	−63	38		3.3
Inf. frontal s.	9/45									35	19	29		3.1
Sup. frontal s.	8/9									34	40	35		3.1
Inf. frontal s. (#10)	45/9									**36**	**21**	**21**		3.0
Mid. frontal g.	46									32	41	3		3.0

Note. Brodmann's areas, Talairach coodinates, and the *P* values (in exponents, base 10) for activation at the local maxima are given. The numbers in parentheses following the anatomic localizations in bold type refer to the hemodynamic response graphs in Fig. 2 and 3. s., sulcus; g., gyrus; lat., lateral; sup., superior, inf., inferior; asc., ascending; des., descending; ant., anterior; post, posterior; mid., middle; med., medial

formed consent after the experimental procedures had been fully explained. The protocol complied with the Declaration of Helsinki and was approved by the Human Research Committee of Massachusetts General Hospital.

Tasks

Experimental tasks were controlled by a Macintosh PowerPC using Macintosh stimulus presentation software (MacStim®). Prior to scanning, subjects practiced until they understood the tasks. They were instructed to respond as quickly and accurately as possible and were informed that they would be paid a $.15 bonus for each correct response. Stimuli were projected onto a screen positioned on the head coil. Subjects responded by pressing a keypad with their thumbs on either hand. Response time (RT) and side (right or left) were recorded.

Each WM trial began with a central fixation cross for 500 ms followed by the presentation of a set of five digits (targets) to be learned (3500 ms) (Encode) (Fig. 2). This was followed by the Delay epoch during which time the screen was blank. During the Probe epoch, subjects were presented with a single digit (probe) for 2000 ms. In half the trials the probe was a target (a member of the memorized set) and in half the trials the probe was a foil (not a member of the memorized set). Subjects responded by pressing a button box with their right thumb for targets and their left

thumb for foils. The three trial types differed only in the length of the delay period that lasted either 0" (D0), 2" (D2), or 4" (D4). The three trial types randomly alternated with a fixation baseline condition within each run. During the baseline condition, subjects fixated on an asterisk that appeared in the center of the screen. The duration of fixation randomly varied in increments of 2 s up to a maximum of 12". The schedule of events was determined using a technique to optimize the statistical efficiency of event-related designs (Dale, 1999). Subjects performed six runs of 4 min 48 s each. Each run contained nine trials of each WM condition and 72 s of fixation. The total experiment time was approximately 35 min.

Image acquisition

Anatomical and functional data were collected with a 3.0 Tesla Allegra Medical System Magnetom imaging device modified for echoplanar imaging (Siemens Medical System, Iselin, NJ). Head stabilization was achieved with cushioning and a forehead strap and all subjects wore earplugs to attenuate noise. Automated shimming procedures were performed and scout images were obtained. Two high resolution 3D MPRAGE sequences (TR/TE/Flip = 6.6 ms/3 ms/ 8°) with an in-plane resolution of 1 and 1.3 mm slice thickness were collected in the sagittal plane for spatial normalization (Talairach and Spherical) and for slice pre-
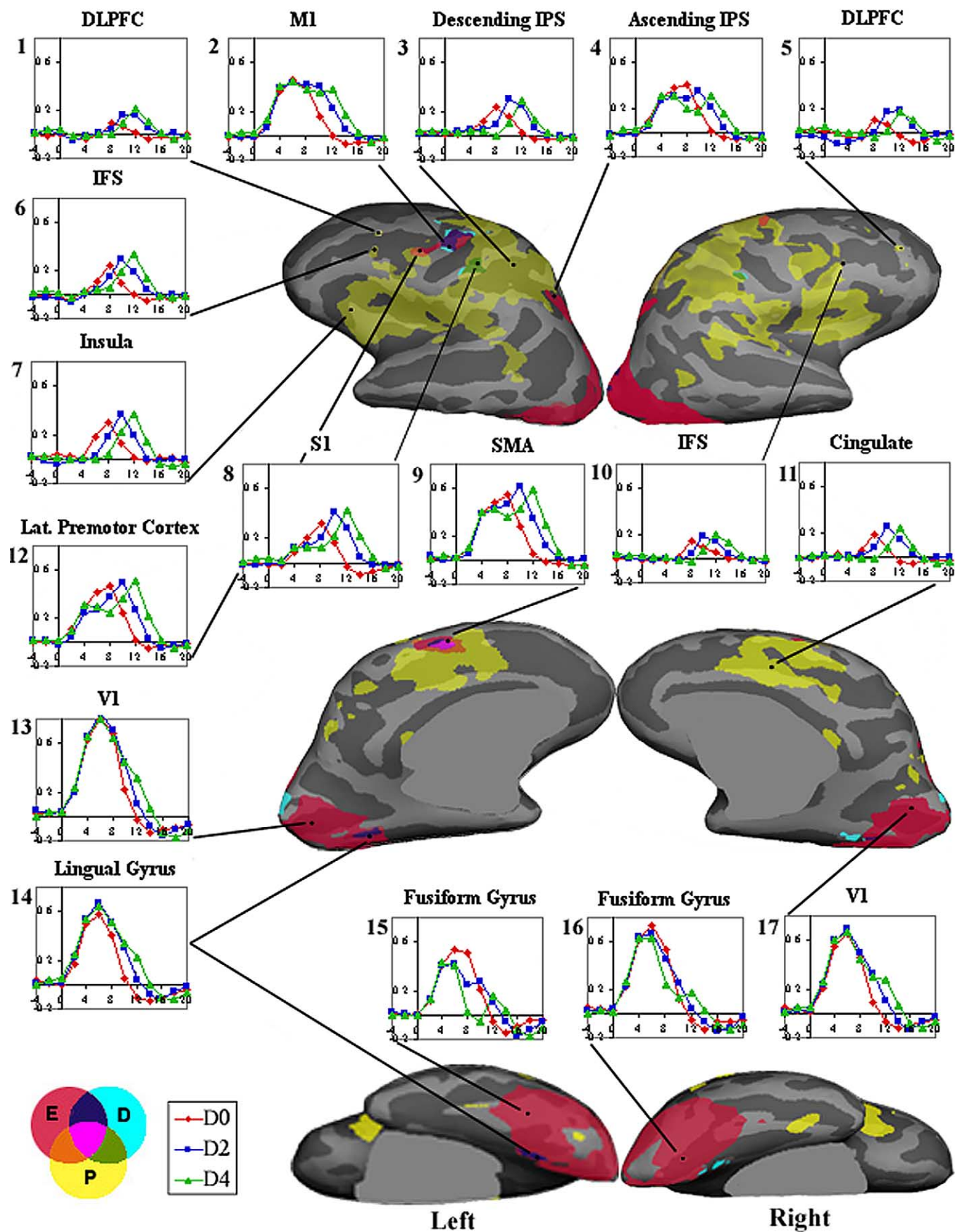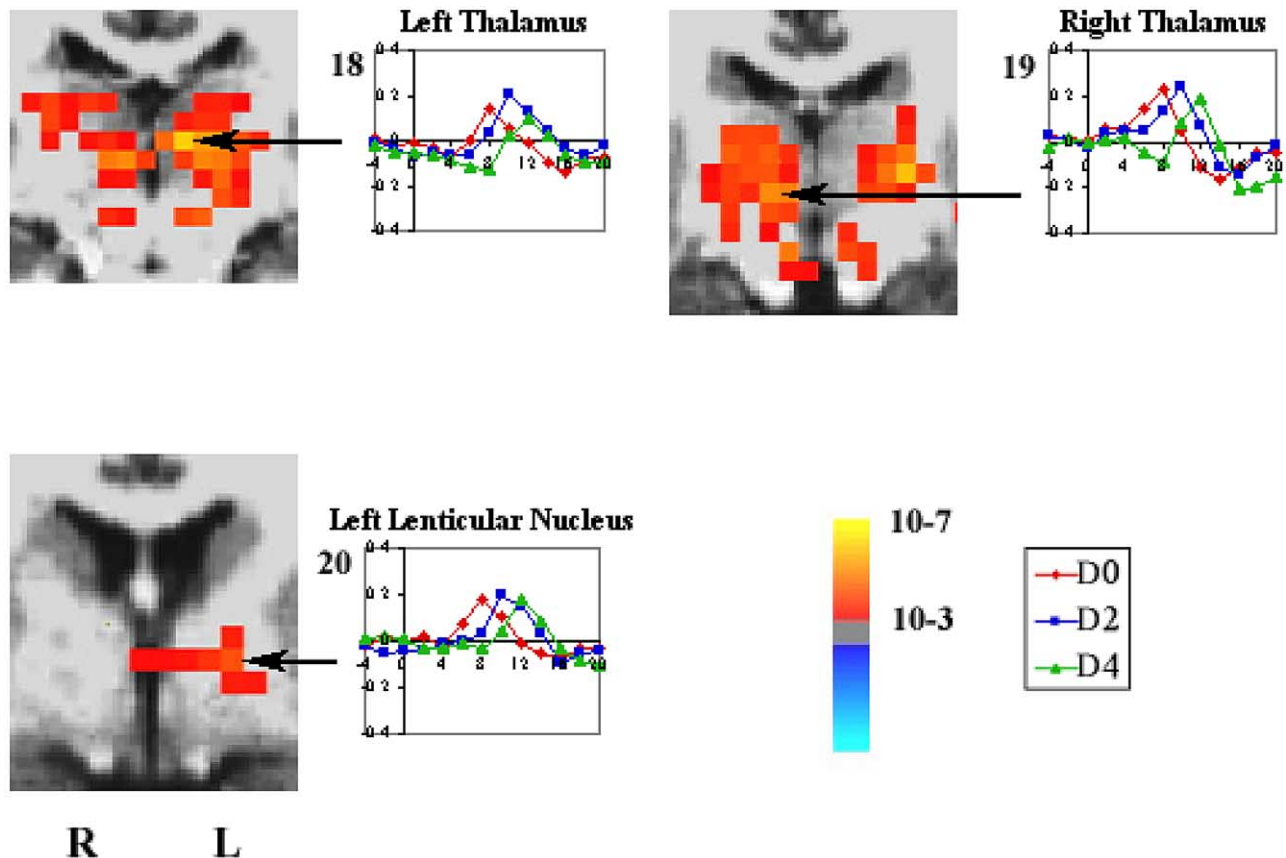
Fig. 4. Statistical maps of subcortical activation in the Probe contrast displayed on Talairach transformed coronal sections. The HDR time course graphs for voxels with peak activation in thalamus and lenticular nucleus are displayed. Time in seconds is on the *x* axis and percent signal change relative to the fixation baseline (range: −0.4 to 0.4) is on the *y* axis. The HDRs for D0 trials are represented by red lines, D2 by blue lines, and D4 by green lines. The numbering of the HDR graphs corresponds to the locations described in the text and in Table 1.

scription. T1 and T2 sequences were gathered to assist in the registration of the functional data to the high-resolution anatomical scans. Functional images were collected using Blood Oxygen Level Dependent (BOLD) contrast and a gradient echo T2* weighted sequence (TR/TE/Flip = 2000 ms/30 ms/90°) to measure variations in blood flow and oxygenation. Twenty contiguous horizontal 6 mm slices parallel to the intercommissural plane (voxel size 3.13 × 3.13 × 6 mm) were acquired interleaved. Four images at the beginning of each scan were acquired and discarded to allow longitudinal magnetization to reach equilibrium.

fMRI data analysis

Functional scans were corrected for motion using the AFNI algorithm (Cox and Jesmanowicz, 1999) to align each

scan to the first image of the first functional scan. The data were normalized by scaling the whole brain signal intensity to a fixed value of 1000. FIR estimates of the event-related hemodynamic responses were calculated for each trial type (D0, D2, D4) within subjects. This involved using a linear model to estimate the average signal intensity at each of 13 time points with an interval of 2 s (corresponding to the TR) ranging from 4 s prior to trial onset to 20 s posttrial onset. Temporal correlations in the noise were accounted for by prewhitening using a global estimate of the residual error autocorrelation function truncated at 30 s. The details of this analysis are presented elsewhere (Burock and Dale, 2000). Functional images were aligned to the 3D structural image for that subject. This image was created by motion-correcting and averaging the two MPRAGE scans. In preparation for group averaging, the functional and anatomical data

Fig. 3. Cortical activation for each WM epoch displayed on lateral, medial, and inferior views of the inflated cortical surface. Vertices significantly activated in the Encode contrast are displayed in red, Delay in blue, and Probe in yellow. The color scheme for vertices activated in more than one contrast is illustrated in the lower left corner. The gray masks cover nonsurface regions in which any activation is displaced. The HDR time course graphs for vertices with peak activation are displayed for selected regions. Time in seconds is on the *x* axis and percent signal change relative to the fixation baseline (range: −0.2 to 0.8) is on the *y* axis. The HDRs for D0 trials are represented by red lines, D2 by blue lines, and D4 by green lines. The numbering of the HDR graphs corresponds to the locations described in the text and in Table 1.

were smoothed using a 3D 8 mm FWHM Gaussian kernel, spatially normalized using Talairach transformation (Collins et al., 1994; Talairach and Tournoux, 1988) and a surface-based spherical coordinate system (Dale et al., 1999; Fischl et al., 1999a, 1999b). Following spatial normalization, the significance of each contrast was tested using a random effects model in which the mean and standard error of the contrast effect size (i.e., differences between hemodynamic response estimates for the conditions being compared) were computed across subjects. Activation in cortical regions was localized using the surface-based spherical system and subcortical activation was localized in Talairach space. Talairach coordinates for cortical activation were derived from the spherical maps to allow comparison with other studies.

In order to draw inferences about the regional activity associated with Encode, Delay, and Probe epochs, we constructed contrasts using the results of the FIR estimates. We identified active regions using an uncorrected significance threshold of $P \leq .001$. For each region identified as active by the contrasts we examined the time course of the HDR in the vertex (on surface maps) or voxel (in Talairach maps) with the peak task-related signal change, scaled by the error variance. The HDRs were derived from the FIR models.

Encode

Because Encode is the first component of the trial in the FIR models, it is not affected by hemodynamic overlap from previous components. For this reason, identifying the associated regional activity is relatively straightforward. We compared the amplitudes from the FIR estimates at 4 s following the onset of each trial to the fixation baseline condition (Fig. 2a). This time point was selected to represent peak encode activation uncontaminated by the start of the Delay or Probe epochs. Based on previous observations in primary visual cortex, the HDR to a stimulus starts to rise about 2 s after stimulus onset and peaks between 4 and 7 s (Boynton et al., 1996; Dale and Buckner, 1997; Savoy, 2001).

Delay

Activity related to the Delay epoch was identified by computing the difference between the averaged responses to the D0 and D4 trials averaged across all of the time points (Fig. 2b). The rationale for this is that the D0 and D4 trials have identical Encode and Probe components that will cancel each other in the difference of the averages leaving only activity due to Delay. In this way we isolate Delay activity without assuming any shape to the HDR.

We also computed an independent "omnibus" contrast. This contrast uses F-tests of the FIR estimates at each time point to identify task-related activation due to any event or combination of events relative to fixation. We used the omnibus contrast to ensure that our delay contrast was not insensitive to DLPFC activation during the delay epoch by

examining the HDRs of each DLPFC vertex that was activated at any time point during the WM trials.

Probe

Because the Probe epoch always follows the Encode and Delay epochs, activation present during the Probe epoch may also represent residual activation due to encoding and maintenance. To identify regions that were significantly associated with Probe, we constructed a contrast to determine which regions were significantly more active at 12 vs 8 s posttrial onset in the D4 trials (Fig. 2c). Activation at 8 s posttrial onset, which occurs 4 s after the start of Delay and immediately prior to the probe onset, represents peak Delay and residual Encode activation. Activation at the 12 s time point, in addition to peak Probe activation, may represent residual Encode and Delay activation, but to a lesser extent than is present at the 8 s time point. Consequently, any positive difference between 12 and 8 s posttrial onset can only be due to activity associated with Probe, except for the case where there are deactivations during Delay. We inspected the HDRs of all the regions identified by this contrast to confirm that they were not an artifact of deactivation during Delay. In regions that did show a deactivation during Delay, we examined whether they were also active in an alternate Probe contrast (Fig. 2d). This contrast identifies regions that were more active at 8 vs 4 s posttrial onset in the D0 trials which do not include a Delay epoch. In regions activated during Delay and, to a lesser extent, during Encode, our primary Probe contrast, using D4 trials, may underestimate the significance of Probe activation.

Results

Performance

A repeated measures ANOVA revealed no effect of the delay length on accuracy (percent correct: F(2,11) = .21, P = .81; D0 = 97.2% ± 2.8; D2 = 96.6% ± 2.6; D4 = 96.8% ± 2.6). A randomized block ANOVA with subjects as the random factor similarly showed no effect of the delay length on RT (F(2,11) = .99, P = .38; D0 = .892 ± .308; D2 = .902 ± .304; D4 = .882 ± .309).

Activation

Table 1 provides the localizations, Talairach coordinates, and corresponding Brodmann's areas for the vertex (or voxel for subcortical regions) with peak task-related signal change for regional activation associated with each epoch. In several instances, the cortical surface and Talairach localizations do not correspond. This is a by-product of the differing methodologies. The Talairach procedure used in this study (Collins et al., 1994) computes a 12 parameter transform that optimally aligns the individual subject's high resolution T1-weighted anatomical image with that of an

atlas. While this type of procedure accurately aligns sub-cortical structures, it does not, in general, align corresponding cortical folds across individuals (Fischl et al., 1999b). For example, the anterior and posterior banks of the central sulcus are difficult to distinguish based solely on their Talairach coordinates (Fischl et al., 1999b). In contrast, the surface maps use a nonrigid alignment based on cortical geometry. Unlike intensity-based techniques, this method explicitly aligns cortical folding patterns across individuals. For this reason, the surface maps provide more accurate intersubject registration of cortical regions than the standard linear Talairach transformation (Fischl et al., 1999b). Fig. 3 displays cortical activation for each WM epoch on the inflated surface. Fig. 4 displays statistical maps of subcortical activation from the Probe contrast. The HDR time courses for peak activation in selected regions are displayed. In the descriptions of regional activation that follow, the numbers in parentheses following the "#" symbol correspond to the number of the HDR time courses in Figs. 3 and 4.

Encode

The Encode epoch was associated with activation in a fairly symmetrical network of regions. These included bilateral primary visual (V1, BA 17: #13, #17) and visual association cortices in the occipital and inferior temporal lobes including the fusiform gyrus (BA 18 and 19: #15, #16) and the ascending segment of the intraparietal sulcus (IPS, BA 7/40: #4). Examination of the HDRs indicates that although these regions were active during encode, they also responded to the onset of the probe, albeit to a lesser, nonsignificant extent. The smaller Probe response in these regions is not surprising because the probe was presented for 2 rather than 4 s and consisted of one rather than five digits. Activation in primary motor cortex (BA 4: #2), lateral premotor cortex (BA 6: #12), and the supplementary motor area (SMA, BA 6: #9) of the left-hemisphere were associated with all three epochs.

Delay

The Delay epoch was associated with activation in bilateral visual association areas in the occipital and temporal lobes including the lingual gyrus (BA 19: #14), and bilateral primary sensory cortex (BA 2: #8). Delay-related SMA (BA 6: #9), primary motor (BA 4: #2), and lateral premotor activity (BA 6: #12) was exclusively in the left hemisphere. Examination of the HDRs for all of the activated regions reveals that none was activated exclusively during Delay. There was no DLPFC activity associated with Delay, even in a more liberal fixed effects analysis with a threshold of $P < .01$. To be certain that our failure to find DLPFC activation during the delay was not due to the limitations of this particular contrast, we also examined the HDRs of DLPFC activation in the omnibus contrast. The locations of active DLPFC vertices that were identified by this contrast were similar to those identified in the probe contrast (below) and

their HDRs remained at or near baseline during the time points corresponding with the delay.

Probe

The Probe epoch was associated with the most widespread activation. Activation in motor and premotor cortex was fairly symmetrical. Activity in several cortical regions was uniquely associated with Probe as determined by both the contrast maps and the HDR time courses. These regions include the descending segment of the IPS (BA 2/40: #3), insula (#7), cingulate gyri, and sulci (BA 32/24: #11), inferior frontal gyri and sulci (IFG/S, BA 44/45: #6, #10), and DLPFC (BA 9/46: #1, #5). In addition, only Probe was associated with subcortical activation in the thalamus and lenticular nucleus (Fig. 3). Examination of the HDR time courses for the subcortical regions revealed that Delay was associated with bilateral thalamic deactivation (subthreshold in the delay contrast), but no change from baseline in the lenticular nucleus. The deactivation during Delay leads to an overestimation of thalamic activation in the Probe contrast. We confirmed that the thalamic activation identified by the Probe contrast was not an artifact of this deactivation with our alternate Probe contrast (Fig. 2d). This contrast revealed significant activation in the same thalamic regions. Because there is no convincing deactivation during Encode, this finding confirms the association of thalamic activation with the Probe epoch.

Discussion

Significant activation was detected in a network of regions that was previously identified in several block design studies of the SIRP (Manoach et al., 1997, 1999, 2000; Rypma et al., 1999) and that have been associated with WM performance in a range of tasks (Cohen et al., 1997). The current event-related study provides a window on their behavioral affiliations. The findings were generated using a method that makes no a priori assumptions about the shape of the HDR. Thus, the potential to misattribute activity to adjacent epochs was minimized. Activation in the DLPFC, thalamus, and basal ganglia was exclusively associated with the Probe. This is consistent with previous neuroimaging and lesion studies that suggest that the DLPFC plays a greater role in preparing a response based on information stored in WM than in storage itself (e.g., Petrides, 2000; Rowe and Passingham, 2001; Rowe et al., 2000). Moreover, the findings suggest that frontostriatal circuitry plays a role in response processes.

The Encode, Delay, and Probe epochs were associated with overlapping but distinct patterns of brain activation. With the exception of sensorimotor regions, which showed greater left-hemisphere activation in Encode and Delay, the activation patterns were largely symmetrical. Encoding was most strongly associated with widespread activation in V1 and visual association cortex. The Delay epoch was associ-

ated with activation in downstream visual association areas bilaterally; bilateral primary sensory cortex; and primary motor and premotor regions of the left-hemisphere. None of these regions was uniquely involved in Delay and many, including primary motor cortex, the SMA and lateral premotor cortex, were involved in all three epochs, consistent with previous findings (Chein and Fiez, 2001). This suggests that they either support diverse cognitive demands or that performance in all three epochs relies on similar underlying processes that are subserved by these regions. The Probe epoch was associated with the most widespread activation. And activity in many regions, including the DLPFC, IFS, IPS, cingulate, insula, thalamus, and basal ganglia, was uniquely associated with the Probe epoch.

The exact contribution of the DLPFC to WM is a topic of ongoing debate. Single unit recording studies of delayed-response tasks in monkeys find that DLPFC neurons are persistently active during the delay (e.g., Funahashi et al., 1989; Fuster, 1973). In the typical spatial delayed-response task, the expected motor response is determined at the initial stimulus presentation and is therefore known during the delay. For this reason, it is not clear whether the delay activity of DLPFC neurons reflects maintenance or response preparation (e.g., the animal can plan the saccade to a remembered location prior to the onset of the response cue). Recent work addressing this ambiguity suggests that the DLPFC has neurons engaged in two separate processes during the delay—maintaining a constant sensory representation and response preparation that increases toward the onset of a saccade (Constantinidis et al., 2001; Quintana and Fuster, 1999). This suggests DLPFC involvement in both maintenance and response preparation during the delay epoch.

Neuroimaging studies that attempt to identify activation specifically associated with the delay epoch are divided with regard to both the presence and the role of DLPFC activity. The DLPFC is consistently found to be active during delay periods that require manipulative processes but is variably active during those that emphasize maintenance. Maintenance refers to holding information "on-line" in the mind's eye in the absence of external stimuli. Manipulation refers to the operations conducted on this information such as updating, reordering, monitoring and temporal tagging. Maintenance and manipulation may not be entirely dissociable because, especially at higher WM loads, maintenance may require strategic processing (D'Esposito et al., 1998).

While some studies do not find DLPFC activity during a delay periods that emphasize maintenance (Rowe and Passingham, 2001; Rowe et al., 2000), many others do (Chein and Fiez, 2001; Courtney et al., 1997; Leung et al., 2002; Rypma and D'Esposito, 1999). Task attributes that may determine whether DLPFC is engaged during the delay period of tasks that emphasize maintenance include the level WM load, whether response preparation is required, and the type of material being maintained. Rypma and colleagues studied the DLPFC contribution to WM using

both event-related and block design versions of the SIRP and by varying WM load (Rypma and D'Esposito, 1999; Rypma et al., 1999). They interpreted their findings of DLPFC activation at higher WM loads to suggest that DLPFC activity during the delay is related to strategic processes used to manage high capacity loads and not to maintenance of information per se. Several studies comparing delay epochs with and without manipulative requirements report that although the DLPFC is active during maintenance, it is significantly more active when manipulation is also required (Wagner et al., 2001), even when the tasks are matched for difficulty (D'Esposito et al., 1999; Postle et al., 1999). One study reported DLPFC activity when subjects had to prepare a sequential action during the delay, but not during simple maintenance (Pochon et al., 2001). However, another study found that DLPFC activity was present during maintenance even when no decision or response was required (Wagner et al., 2001). DLPFC may also be preferentially engaged in maintenance of spatial materials (Leung et al., 2002). In summary, DLPFC activity is sometimes shown to be temporally associated with delays that emphasize maintenance, but has a greater response with high WM loads and when manipulation and response preparation are required.

The Delay epoch of the current paradigm required very little or no strategic processing given the relatively low WM load of five digits. It also did not allow for the preparation of a *specific* response. There was an equal probability of having to make a right or left trigger press and the required response was not determined until the probe onset, the timing of which was unpredictable given the random sequence of trials. Thus, the primary requirement of the Delay was simple maintenance of a set of target digits for several seconds. In this context, there was no evidence of DLPFC activity. Rather, the timing of DLPFC activity corresponded to the onset of the Probe. This suggests that for WM tasks requiring simple maintenance of nonspatial materials DLPFC activation is primarily associated with a subset of the cognitive processes that are initiated by the probe. These may include mentally scanning the items maintained in WM, comparing them to the probe, making a binary decision (target or foil?), and selecting the appropriate motor response. This is consistent with a previous finding that the rate of mental scanning is directly related to DLPFC activation during the probe and not during the delay (Rypma and D'Esposito, 1999). (The slope of the regression line of RT plotted by the number of targets in the memorized set provides an index of the rate of mental scanning in the SIRP (Sternberg, 1966, 1969, 1975).

It is possible that this study lacked sufficient power to detect meaningful DLPFC activity during the delay either due to the use of an event-related design, the use of an FIR model, or an undershoot in response to the Delay epoch. It is important to note, however, that there was no DLPFC activity in the Delay contrast even at a reduced threshold in a more liberal analysis. In addition, examination of the HDR

time courses of DLPFC activation in the omnibus contrast (which is not biased to any one epoch), demonstrates that DLPFC activity stays close to the baseline until the onset of the probe. While we cannot claim that there is no delay-related activation in the DLPFC because our method may not have been sufficiently sensitive, our findings are consistent with previous studies in suggesting that DLPFC activation is primarily associated with the response to a probe rather than simple maintenance (Petrides, 2000; Rowe and Passingham, 2001; Rowe et al., 2000).

Another possible limitation to the Delay contrast is that it rests on the assumption that the only difference between trials with a 0 s and a 4 s delay is the delay period. This assumption is that of "pure insertion"—the idea that a cognitive process can be added to a preexisting set of processes without affecting them (c.f., Zarahn et al., 1997). While there is no reason to expect the Encode epoch to differ between these two trial types because it occurs prior to the delay, it is possible that the response to the probe was affected by delay length. This is suggested by reports that the DLPFC response to a probe is greater in a delay vs a "no-delay" condition (Zarahn et al., 1997, 1999). However, in these studies, the response requirements of the no-delay and delay conditions were different. In the no-delay condition the target and probe were presented together on the screen and therefore the response required visual discrimination. In the delay condition, the target and probe were presented sequentially and the response was guided by WM. Thus, the differential activation of the DLPFC during the probe may reflect these different processing requirements rather than the presence vs. absence of a delay. In the present study, the targets and probes were presented sequentially for all three trial types and they did not overlap. And in all three trial types the response to the probe likely required the same processes—the mental scanning of the contents of WM, a comparison, a binary decision, and selection of a motor response (Sternberg, 1966). The finding that RT did not differ across the three WM trial types is consistent with the notion that they required the same processes. (Accuracy was at ceiling levels in all conditions and thus, was not sensitive to potential differences between conditions.) Even if the length of the delay did interact with the probe response in the DLFPC, this would have biased the delay contrast in favor of finding DLPFC activity rather than against it.

In addition to the DLPFC, the Probe epoch was exclusively associated with activation in the thalamus and basal ganglia. In our previous block design study of the SIRP, basal ganglia and thalamic activation was seen in subjects with schizophrenia, but not in healthy subjects (Manoach et al., 2000). Several block-design neuroimaging studies of healthy subjects report basal ganglia and thalamic activation under conditions of increased WM demand (Barch et al., 1997; Callicott et al., 1999; Goldberg et al., 1998; Rypma et al., 1999). The variable-set SIRP of the present study was more challenging than the fixed-set SIRP of our previous

work (RTs for healthy subjects were significantly higher at the same WM load: .892 ± 0.31 vs .787 ± 0.26). This increased demand might explain the appearance of these regions in healthy subjects.

Additional evidence that frontostriatal neural circuitry participates in WM is provided by single unit recordings and lesion studies in animals (Apicella et al., 1992; Battig et al., 1960) and lesion and dysfunction studies in humans (Owen et al., 1997; Partiot et al., 1996). However, the role of this circuitry in WM is not understood. During the delay periods of delayed-response tasks, striatal neurons exhibit sustained activity that closely resembles that of the DLPFC (Apicella et al., 1992). Such findings have led to the hypothesis that this circuitry plays a role in maintaining tonic activity of the DLPFC during maintenance periods in which information critical to a correct response is held "on line" (Goldman-Rakic, 1995; Levy et al., 1997). Positive feedback in these reverberating loops has been hypothesized to provide a mechanism for sustaining WM (Beiser and Houk, 1998). In contrast, we found frontostriatal activity to be associated exclusively with the Probe epoch. This suggests that activity in frontostriatal circuitry may also reflect processes related to selecting an appropriate response based on the contents of WM.

In the present study the DLPFC activation observed was less extensive than Probe activity in other regions. In our previous block design studies of the SIRP, we reported more extensive DLPFC activation, but could not examine its temporal dynamics (Manoach et al., 1997, 1999, 2000). Our block design format used a "fixed set" SIRP design. In the fixed set version, there is one memory set followed by multiple probes presented in a rapid succession (less than 3 s apart). This design emphasizes processes related to the probe to a far greater extent than the "variable set" design of the current study in which each memory set is followed by only one probe. In addition, in the fixed set design, the targets must be held on-line despite intervening probes that serve as distractors. While other areas of the cortex, particularly extrastriate visual areas, are capable of sustaining a response to a brief stimulus for periods up to several seconds (Miller et al., 1996), the ability to support sustained activity in the face of interference is thought to be one of the distinguishing characteristics of the DLPFC (Miller and Cohen, 2001; Sakai et al., 2002). It may be that given the requirement of simple maintenance in the absence of distractors, other regions, including visual association areas, were sufficient to maintain information during the delay of this variable set SIRP. This is consistent with the finding that monkeys with prefrontal lesions can perform delayed-response tasks accurately in the absence of distractions (Malmo, 1942). In summary, the decreased emphasis on the probe and the absence of distractors may contribute to the lack of a DLPFC response during the delay and the more restricted pattern of DLPFC activation during the probe epoch.

Finally, the asymmetry of the motor findings during the

Encode and Delay epochs deserves comment. This activity was primarily on the left, even though no movement was required. During the Probe epoch, when right and left manual responses were equally frequent, motor activation was bilateral. For the reasons discussed above, the left-sided activity during Encode and Delay, is unlikely to represent the formation of a specific motor plan. But it may represent the anticipation of making a motor response. The HDR time courses of these regions (Fig. 2: #2, #9, and #12) reveal an increase during Encode and a plateau during Delay. This activity may be akin to the "readiness potential" in the event-related potential literature. The readiness potential refers to endogenously driven, rather than stimulus driven, brain activity over central sulcus sites that precedes an impending voluntary movement (Kutas and Dale, 1997). It is generally found to be greater over contralateral sites. In the context of an unpredictable response side, the left-hemisphere activation suggests that subjects were primed to respond to a target rather than a foil (subjects responded to targets with their right hand). In the SIRP, targets are found to have faster RTs than foils (Sternberg, 1966, 1969, 1975) although, surprisingly, there was no difference in the present study. In a previous study of the SIRP we found shorter RTs to targets than foils and greater left-sided motor activation (Manoach et al., 1997). The shorter RTs are unlikely to represent a simple handedness effect because there was no difference in RT for the right and left hands in the visually guided control task.

While this discussion has focussed primarily on the DLPFC, thalamus, and basal ganglia, the table and figures reveal that an extensive network of regions is associated with the performance of even a relatively simple WM task. A division of the task into Encoding, Delay, and Probe epochs gives rise to distinct, but overlapping patterns of neural activity. These findings are consistent with the view that there is not a one-to-one mapping of particular processes in a particular region, rather, multiple brain regions interact in complex ways depending on the particular task requirements (Carpenter et al., 2000).

Limitations of the methods employed include that both the encode and probe time points are compared to fixation and for this reason visual and motor activity do not cancel out. However, even when baseline tasks with identical sensorimotor requirements are employed, the associated activity may not completely cancel out due to the interaction between sensorimotor and cognitive task requirements (e.g., the assumption of pure insertion may be violated). Also, although we have identified activity associated with each epoch, our method does not allow us to directly compare this activity. Finally, encoding information, maintaining it over a delay and using this information to respond to a probe can probably all be further broken down into cognitive subprocesses, some of which are probably shared in common and others that are distinct. The current study identifies patterns activity during different epochs, but does not isolate these cognitive subprocesses. Future work might

productively focus on identifying the neural correlates of the basic processes underlying task performance by manipulating task demands and/or using methods with better temporal resolution.

Conclusions

In this study we used unbiased estimates of HDRs to identify neural circuitry involved in the temporally segregated components of a WM paradigm. The paradigm emphasized maintenance rather than manipulative processes, used a subcapacity WM load, used nonspatial materials, did not introduce distractors during maintenance, and did not provide sufficient information for planning a specific motor response prior to the appearance of the probe. Each of the factors that were minimized in the current study—manipulation, high WM loads, spatial WM demands, distractors, and response preparation—has been associated with DLPFC activity during delays in previous studies. In the current study, there was no evidence of DLPFC activity during the delay. While this may reflect a lack of sensitivity of the current measurements, it is also plausible that activation in other regions may be sufficient for simple maintenance over the span of several seconds. In contrast to the delay, activity in the DLPFC, thalamus, and basal ganglia was associated with the probe epoch. This finding is consistent with the hypothesis that frontostriatal neural circuitry is involved in selecting an appropriate motor response based on the contents of WM. Task manipulations and methods with better temporal resolution will be necessary to identify individual cognitive processes that occur during the Encode, Delay, and Probe epochs of WM tasks and their associated neural activity.

Acknowledgments

References

Apicella, P., Scarnati, E., Ljungberg, T., Schultz, W., 1992. Neuronal activity in monkey striatum related to the expectation of predictable environmental events. J. Neurophysiol. 68, 945–960.

Barch, D.M., Braver, T.S., Nystrom, L.E., Forman, S.D., Noll, D.C., Cohen, J.D., 1997. Dissociating working memory from task difficulty in human prefrontal cortex. Neuropsychologia 35, 1373–1380.

Battig, K., Rosvold, H.E., Mishkin, M., 1960. Comparison of the effect of frontal and caudate lesions on delayed response and alternation in monkeys. J. Comp. Physiol. Psychol. 53, 400–404.

Beiser, D.G., Houk, J.C., 1998. Model of cortical-basal ganglionic processing: encoding the serial order of sensory events. J. Neurophysiol. 79, 3168–3188.

Blair, J.R., Spreen, O., 1989. Predicting premorbid IQ: a revision of the National Adult Reading Test. Clin. Neuropsychologist 3, 129–136.

Boynton, G.M., Engel, S.A., Glover, G.H., Heeger, D.J., 1996. Linear systems analysis of functional magnetic resonance imaging in human V1. J. Neurosci. 16, 4207–4221.

Burock, M.A., Dale, A.M., 2000. Estimation and detection of event-related fMRI signals with temporally correlated noise: a statistically efficient and unbiased approach. Hum. Brain Mapp. 11, 249–260.

Callicott, J.H., Mattay, V.S., Bertolino, A., et al., 1999. Physiological characteristics of capacity constraints in working memory as revealed by functional MRI. Cereb. Cortex 9, 20–26.

Carpenter, P.A., Just, M.A., Reichle, E.D., 2000. Working memory and executive function: evidence from neuroimaging. Curr. Opin. Neurobiol. 10, 195–199.

Chein, J.M., Fiez, J.A., 2001. Dissociation of verbal working memory system components using a delayed serial recall task. Cereb. Cortex 11, 1003–1114.

Cohen, J.D., Perlstein, W.M., Braver, T.S., et al., 1997. Temporal dynamics of brain activation during a working memory task. Nature 386, 604–608.

Collins, D.L., Neelin, P., Peters, T.M., Evans, A.C., 1994. Automatic 3D intersubject registration of MR volumetric data in standardized Talairach space. J. Comput. Assist. Tomogr. 18, 192–205.

Constantinidis, C., Franowicz, M.N., Goldman-Rakic, P.S., 2001. The sensory nature of mnemonic representation in the primate prefrontal cortex. Nat. Neurosci. 4, 311–316.

Courtney, S.M., Ungerleider, L.G., Keil, K., Haxby, J.V., 1997. Transient and sustained activity in a distributed neural system for human working memory. Nature 386, 608–611.

Cox, R.W., Jesmanowicz, A., 1999. Real-time 3D image registration for functional MRI. Magn. Reson. Med. 42, 1014–1018.

D'Esposito, M., Aguirre, G.K., Zarahn, E., Ballard, D., Shin, R.K., Lease, J., 1998. Functional MRI studies of spatial and nonspatial working memory. Cogn. Brain Res. 7, 1–13.

D'Esposito, M., Postle, B.R., Ballard, D., Lease, J., 1999. Maintenance versus manipulation of information held in working memory: an event-related fMRI study. Brain Cogn. 41, 66–86.

Dale, A.M., 1999. Optimal experimental design for event-related fMRI. Hum. Brain Mapp. 8, 109–114.

Dale, A.M., Buckner, R.L., 1997. Selective averaging of rapidly presented individual trials using fMRI. Hum. Brain Mapp. 5, 329–340.

Dale, A.M., Fischl, B., Sereno, M.I., 1999. Cortical surface-based analysis. I. Segmentation and surface reconstruction. Neuroimage 9, 179–194.

Duann, J.R., Jung, T.P., Kuo, W.J., et al., 2002. Single-trial variability in event-related BOLD signals. Neuroimage 15, 823–835.

Fischl, B., Sereno, M.I., Dale, A.M., 1999a. Cortical surface-based analysis. II: Inflation, flattening, and a surface-based coordinate system. Neuroimage 9, 195–207.

Fischl, B., Sereno, M.I., Tootell, R.B.H., Dale, A.M., 1999b. High-resolution intersubject averaging and a coordinate system for the cortical surface. Hum. Brain Mapp. 8, 272–284.

Funahashi, S., Bruce, C.J., Goldman-Rakic, P.S., 1989. Mnemonic coding of visual space in the monkey's dorsolateral prefrontal cortex. J. Neurophys. 61, 331–349.

Fuster, J.M., 1973. Unit activity in prefrontal cortex during delayed-response performance: neuronal correlates of transient memory. J. Neurophysiol. 36, 61–78.

Goldberg, T.E., Berman, K.F., Fleming, K., et al., 1998. Uncoupling cognitive workload and prefrontal cortical physiology: a PET rCBF study. Neuroimage 7, 296–303.

Goldman-Rakic, P.S., 1995. Toward a circuit model of working memory and the guidance of voluntary motor action, in: Houk, J.C., Davis, J.L., Beiser, D.G. (Eds.), Models of Information Processing in the Basal Ganglia, The MIT Press, Cambridge, MA, pp. 131–148.

Haxby, J.V., Petit, L., Ungerleider, L.G., Courtney, S.M., 2000. Distinguishing the functional roles of multiple regions in distributed neural systems for visual working memory. Neuroimage 11, 380–391.

Jha, A.P., McCarthy, G., 2000. The influence of memory load upon delay-interval activity in a working-memory task: an event-related functional MRI study. J. Cogn. Neurosci. 2 (12 Suppl), 90–105.

Kutas, M., Dale, A., 1997. Electrical and magnetic readings of mental functions, in: Rugg, M.D. (Ed.), Cognitive Neuroscience, MIT Press, Cambridge, MA, pp. 197–242.

Leung, H.C., Gore, J.C., Goldman-Rakic, P.S., 2002. Sustained mnemonic response in the human middle frontal gyrus during on-line storage of spatial memoranda. J. Cogn. Neurosci. 14, 659–671.

Levy, R., Friedman, H.R., Davachi, L., Goldman-Rakic, P.S., 1997. Differential activation of the caudate nucleus in primates performing spatial and nonspatial working memory tasks. J. Neurosci. 17, 3870–3882.

Malmo, R.B., 1942. Interference factors in delayed response in monkeys after removal of frontal lobes. J. Neurophysiol. 5, 295–308.

Manoach, D.S., Schlaug, G., Siewert, B., et al., 1997. Prefrontal cortex fMRI signal changes are correlated with working memory load. Neuroreport 8, 545–549.

Manoach, D.S., Press, D.Z., Thangaraj, V., et al., 1999. Schizophrenic subjects activate dorsolateral prefrontal cortex during a working memory task as measured by fMRI. Biol. Psychiatry 45, 1128–1137.

Manoach, D.S., Gollub, R.L., Benson, E.S., et al., 2000. Schizophrenic subjects show aberrant fMRI activation of dorsolateral prefrontal cortex and basal ganglia during working memory performance. Biol. Psychiatry 48, 99–109.

Miller, E.K., Cohen, J.D., 2001. An integrative theory of prefrontal cortex function. Annu. Rev. Neurosci. 24, 167–202.

Miller, E.K., Erickson, C.A., Desimone, R., 1996. Neural mechanisms of visual working memory in prefrontal cortex of the macaque. J. Neurosci. 16, 5154–5167.

Nystrom, L.E., Braver, T.S., Sabb, F.W., Delgado, M.R., Noll, D.C., Cohen, J.D., 2000. Working memory for letters, shapes, and locations: fMRI evidence against stimulus-based regional organization in human prefrontal cortex. Neuroimage 11, 424–446.

Ollinger, J.M., Corbetta, M., Shulman, G.L., 2001a. Separating processes within a trial in event-related functional MRI: II. Analysis. Neuroimage 13, 218–229.

Ollinger, J.M., Shulman, G.L., Corbetta, M., 2001b. Separating processes within a trial in event-related functional MRI: I. The Method. Neuroimage 13, 210–217.

Owen, A.M., Iddon, J.L., Hodges, J.R., Summers, B.A., Robbins, T.W., 1997. Spatial and non-spatial working memory at different stages of Parkinson's disease. Neuropsychologia 35, 519–532.

Partiot, A., Verin, M., Pillon, B., Teixeira-Ferreira, C., Agid, Y., Dubois, B., 1996. Delayed response tasks in basal ganglia lesions in man: further evidence for a striato-frontal cooperation in behavioural adaptation. Neuropsychologia 34, 709–721.

Petrides, M., 1995. Functional organization of the human frontal cortex for mnemonic processing. Evidence from neuroimaging studies. Ann. NY Acad. Sci. 769, 85–96.

Petrides, M., 2000. Dissociable roles of mid-dorsolateral prefrontal and anterior inferotemporal cortex in visual working memory. J. Neurosci. 20, 7496–7503.

Pochon, J.B., Levy, R., Poline, J.B., et al., 2001. The role of dorsolateral prefrontal cortex in the preparation of forthcoming actions: an fMRI study. Cereb. Cortex 11, 260–266.

Postle, B.R., Berger, J.S., D'Esposito, M., 1999. Functional neuroanatomical double dissociation of mnemonic and executive control processes contributing to working memory performance. Proc. Natl. Acad. of Sci. USA 96, 12959–12964.

Postle, B.R., Zarahn, E., D'Esposito, M., 2000. Using event-related fMRI to assess delay-period activity during performance of spatial and non-spatial working memory tasks. Brain Res. Brain Res. Protoc. 5, 57–66.

Quintana, J., Fuster, J.M., 1999. From perception to action: temporal integrative functions of prefrontal and parietal neurons. Cereb. Cortex 9, 213–221.

Rowe, J.B., Toni, I., Josephs, O., Frackowiak, R.S., Passingham, R.E., 2000. The prefrontal cortex: response selection or maintenance within working memory. Science 288, 1656–1660.

Rowe, J.B., Passingham, R.E., 2001. Working memory for location and time: activity in prefrontal area 46 relates to selection rather than maintenance in memory. Neuroimage 14, 77–86.

Rypma, B., D'Esposito, M., 1999. The roles of prefrontal brain regions in components of working memory: effects of memory load and individual differences. Proc. Natl. Acad. Sci. USA 96, 6558–6563.

Rypma, B., Prabhakaran, V., Desmond, J.E., Glover, G.H., Gabrieli, J.D., 1999. Load-dependent roles of frontal brain regions in the maintenance of working memory. Neuroimage 9, 216–226.

Sakai, K., Rowe, J.B., Passingham, R.E., 2002. Active maintenance in prefrontal area 46 creates distractor-resistant memory. Nat. Neurosci. 5, 479–484.

Savoy, R.L., 2001. History and future directions of human brain mapping and functional neuroimaging. Acta Psychol. (Amst) 107, 9–42.

Sternberg, S., 1966. High-speed scanning in human memory. Science 153, 652–654.

Sternberg, S., 1969. Memory-scanning: mental processes revealed by reaction-time experiments. Am. Sci. 57, 421–457.

Sternberg, S., 1975. Memory scanning: new findings and current controversies. Q. J. Exp. Psychol. 27, 1–32.

Talairach, J., Tournoux, P., 1988. Co-planar Stereotaxic Atlas of the Human Brain. Thieme Medical Publishers, New York.

Wagner, A.D., Maril, A., Bjork, R.A., Schacter, D.L., 2001. Prefrontal contributions to executive control: fMRI evidence for functional distinctions within lateral prefrontal cortex. Neuroimage 14, 1337–1347.

White, K., Ashton, R., 1976. Handedness assessment inventory. Neuropsychologia 14, 261–264.

Zarahn, E., Aguirre, G., D'Esposito, M., 1997. A trial-based experimental design for fMRI. NeuroImage 6, 122–138.

Zarahn, E., Aguirre, G.K., D'Esposito, M., 1999. Temporal isolation of the neural correlates of spatial mnemonic processing with fMRI. Brain Res. Cogn. Brain Res. 7, 255–268.